

Cubic to Tetragonal Phase Transformation in Cold-Compressed Pd Nanocubes

Qixun Guo,^{*,†} Yusheng Zhao,[†] Wendy L. Mao,[‡] Zhongwu Wang,[§] Yujie Xiong,^{||,⊥} and Younan Xia^{||,§}

Los Alamos Neutron Science Center, Los Alamos National Laboratory, Los Alamos, New Mexico 87545, Geological and Environmental Sciences and Photon Science Department, SLAC, Stanford University, Stanford, California 94305, Cornell High Energy Synchrotron Source, Wilson Laboratory, Cornell University, Ithaca, New York 14853, and Department of Chemistry, University of Washington, Seattle, Washington 98195

Received November 29, 2007; Revised Manuscript Received January 16, 2008

ABSTRACT

Pd nanocubes with an average side length of ~ 10 nm were compressed up to 24.8 GPa in a diamond-anvil cell (DAC). In situ synchrotron X-ray diffraction was used to monitor structural changes, and a face-centered cubic (fcc) to face-centered tetragonal (fct) distortion was observed for the first time. This novel discovery not only provides new insights into the pressure-induced behavior of faceted nanocrystals of palladium and other noble metals but also gives guidance for finding new phases in close-packed metals.

Understanding phase transformations in nanocrystal systems is an area of considerable scientific interest.^{1–9} Nanocrystals of group II–VI semiconductors (e.g., CdSe^{1–4} and ZnS^{5–8}) have been used as ideal models for phase transformation studies, which may benefit from the relatively low transformation pressures and temperatures in their extended solids. In contrast, a number of noble metals (e.g., Pd, Pt, Ag, and Au) adopt close-packed configurations and are found to be stable in the face-centered cubic (fcc) structure to extremely high pressure (i.e., at least 77.4, 304, 91.8, and 182 GPa for Pd, Pt, Ag, and Au, respectively¹⁰) at ambient temperature in their extended solids, making it a great challenge to realize their phase transformations. First-principle, total-energy calculations on the tetragonal phases of bulk palladium found that a shallow energy minimum exists for a face-centered-tetragonal (fct)¹¹ state with a small axial ratio of $c/a \approx 0.64$.¹² This tetragonal state was obtained and stabilized in an extremely thin (~ 1.9 nm) Pd film by an epitaxial Bain path.¹³ Recently, Hoffmann et al. investigated the fcc to fct

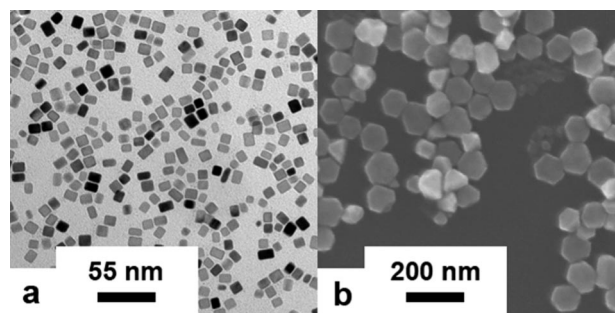


Figure 1. Representative TEM image of the Pd nanocubes (a) and SEM image of the Pd nanoplates (b). The nanocubes are 9 ± 2 nm in edge length and the nanoplates are 50 ± 10 nm in lateral dimensions and 10 ± 2 nm thick. Note that some of the nanocubes are slightly elongated along one edge to become short nanobars.

distortions in transition metals using a tight-binding function, ΔE_{star} .¹⁴ From their theoretical calculations, an fct structure of Pd with $c/a = 0.98$ may be more stable than its related fcc structure. The above theoretical and experimental results motivated us to investigate the possible fcc to fct phase transformations in some faceted nanocrystals of Pd (e.g., nanocubes and nanoplates) at high pressures.

Pd nanocubes with an average side length of ~ 9 nm^{15,16} and hexagonal nanoplates with an average thickness of ~ 10 nm¹⁷ were synthesized using published procedures. Figure 1 shows a representative TEM image of the Pd nanocubes and SEM image of the Pd nanoplates. The as-prepared

* Corresponding author: qxguo@lanl.gov (temporary), guoqixun@ustc.edu (permanent).

[†] Los Alamos National Laboratory.

[‡] Stanford University.

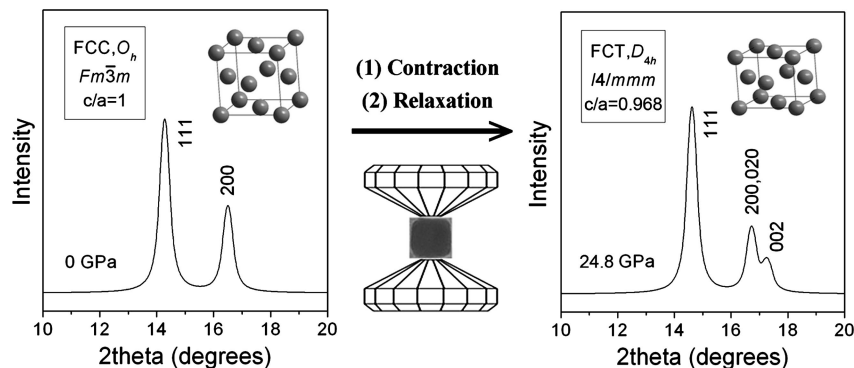
[§] Cornell University.

^{||} University of Washington.

[⊥] Present address: Department of Materials Science and Engineering, University of Illinois at Urbana–Champaign, Urbana, IL 61801.

[§] Present address: Department of Biomedical Engineering, Washington University, St. Louis, MO 63130.

Scheme 1. The Crystal Structures and Simulated X-ray Diffraction Patterns of Both fcc and fct and Their Transformation Processes. To obtain higher contrast, we set c/a as 0.88 ($\ll 0.968$) for fct when we draw the unit cell.



nanocrystals were compressed in a symmetric diamond-anvil cell (DAC) at room temperature and studied in situ using angle-dispersive synchrotron X-ray diffraction.¹⁸ A ruby grain was added for pressure calibration.¹⁹ A previously unknown fcc to fct phase transformation in noble metals was clearly observed at 24.8 GPa in the Pd nanocubes. The crystal structures and simulated X-ray diffraction patterns of both fcc and fct and their transformation processes are depicted in Scheme 1.

Figure 2 shows representative X-ray diffraction patterns for the Pd nanocubes up to 24.8 GPa. It is interesting to note that while the (111) peak clearly shifts to higher 2θ (smaller d -spacing), the (200) peak was relatively incompressible over the increasing pressure range from 0.3 to 9.3 GPa. Figure 3 shows d -spacings and d_{200}/d_{111} values for the Pd nanocubes at pressure from 0.3 to 9.3 GPa. The d_{200}/d_{111} ratio moves further away from the ideal value 0.866 for the fcc structure with increasing pressure, and as pressure exceeds 12.4 GPa, the broadening of the diffraction peaks became very obvious. At pressures >18.8 GPa, a splitting was clearly observed for the (200) peak. Figures 2 and 3

indicate that a displacive phase transformation with a slight deformation in the Pd nanocubes has taken place. At 24.8 GPa, the (200) peak of the pseudo-fcc Pd was fully split into two peaks. The diffraction patterns at this pressure can be indexed as a fct structure with $a = 3.827$ Å, $c = 3.705$ Å, and $c/a = 0.968$.

Figure 4 shows representative X-ray diffraction patterns for the Pd nanoplates up to 20.1 GPa. Both the (111) and (200) peaks had clear shifts to higher 2θ with increasing pressure. The peak broadening is very small, and no peak splitting was observed with a pressure up to the highest value, indicating that the nanoplates were much more stable than the nanocubes at high pressures. This might be related to their difference in crystallinity: nanocubes are single crystals, while nanoplates contain stacking faults in the direction perpendicular to the base plane.

These results bring up a number of questions about the high pressure behavior of Pd nanocubes that need to be explained. Why does the d -spacing of the (002) peak of the nanocubes remain almost a constant over the pressure range from 0.3 to 9.3 GPa? Why does the fcc to fct distortion occur in nanocrystals but not in the bulk solid, and why does this transition occur in nanocubes but not in nanoplates?

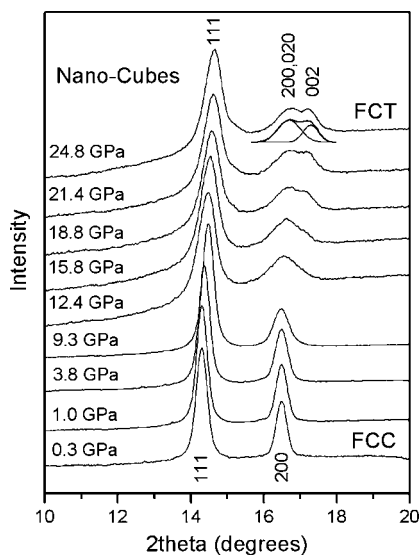


Figure 2. Representative X-ray diffraction patterns for the Pd nanocubes up to 24.8 GPa. The (200) peak of the pseudo-fcc Pd was fully split into two peaks at 24.8 GPa. The diffraction patterns at this pressure can be indexed as a fct structure with $a = 3.827$ Å, $c = 3.705$ Å, and $c/a = 0.968$.

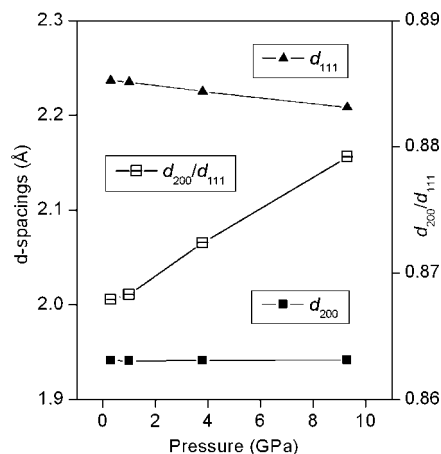


Figure 3. d -Spacings and d_{200}/d_{111} values for the Pd nanocubes at pressures from 0.3 to 9.3 GPa. While the d_{111} value clearly shifts to smaller values with increasing pressure, the d_{200} value remains remarkably constant over this range. This results in a d_{200}/d_{111} ratio that moves away from the ideal value 0.866 for the fcc structure with increasing pressure.

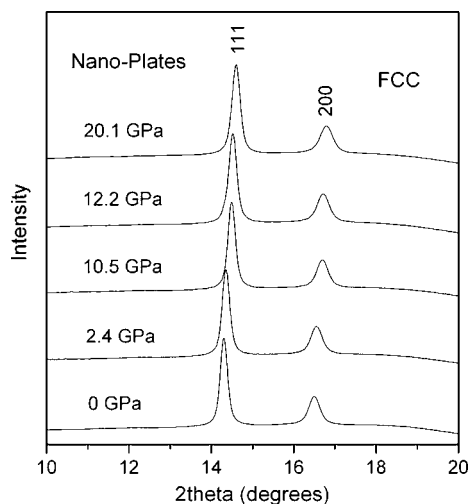


Figure 4. Representative X-ray diffraction patterns for the Pd nanoplates up to 20.1 GPa. The peak broadening is negligible, and no peak splitting was observed with a pressure up to the highest value.

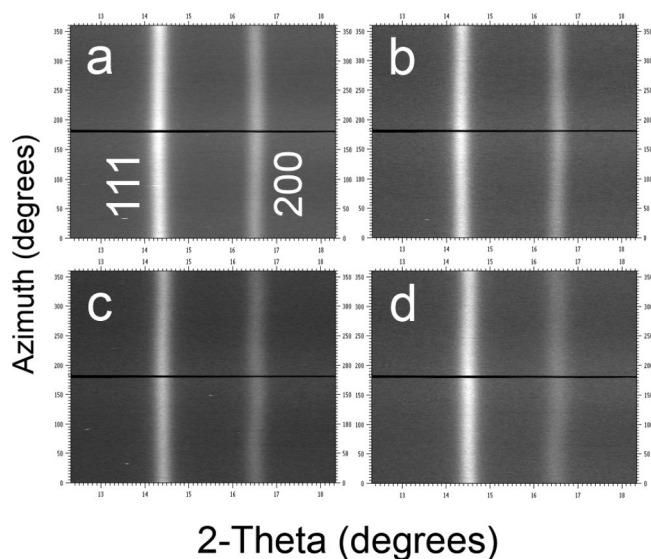


Figure 5. Cartesian (cake) plots of azimuth angle versus 2-theta angle for the Pd nanocubes at different pressures: (a) 0.3 GPa, (b) 1.0 GPa, (c) 3.8 GPa, and (d) 9.3 GPa. The 200 rings at 3.8 and 9.3 GPa appeared wavy and wider areas existed, indicating nonhydrostatic strain conditions even at 3.8 GPa.

Silicone oil is a useful pressure-transmitting medium because it does not dissolve and react with samples and loading it into the DAC is relatively simple.²⁰ It is also able to maintain quasihydrostatic conditions up to ~ 10 GPa if there is enough oil to fully disperse the sample. This was not the case in our experiments where the amount of liquid silicone oil used was relatively small and the nanocubes were not fully dispersed in the pressure medium. Therefore, the nanocubes are not in hydrostatic conditions and shear stresses were present. We unraveled the Debye–Scherrer rings for the Pd nanocubes at $P = 0.3, 1.0, 3.8,$ and 9.3 GPa into Cartesian (cake) plots of azimuth angle versus 2θ angle (Figure 5). The powder diffraction rings at $P = 3.8$ and 9.3 GPa appeared wavy, especially for the 200 rings. In addition, there existed wider areas along the 200 rings at $P = 3.8$ and

9.3 GPa. These results suggest that the Pd nanocubes were in nonhydrostatic strain conditions even at $P = 3.8$ GPa.

According to our X-ray diffraction data (Figures 2 and 3), we proposed a preferential alignment of the [001] direction of the nanocubes parallel to the synchrotron beam and diamond compression axis under nonhydrostatic compression conditions. This preferred orientation makes it difficult to see the diffraction from (002) planes with the intensity in the 200 peak of the pseudo-fcc Pd originating mainly from scattering of the (200) and (020) planes. The external force produced by the two opposing diamond anvils causes the nanocubes to preferentially contract along [001]. The nanocubes will also contract along [100] and [010] because the total volume of the sample decreases under cold compression. It should be noted that the nanocubes are not in mechanical equilibrium in the earliest stages of each compression. So the nanocubes will expand until they reach an equilibrium state along the [100] and [010] directions because the expansion along the [001] direction is almost completely confined by the two opposing diamond anvils. The above relaxation process will result in the observed quasistationary behavior of the 200 and 020 peaks at < 10 GPa. The calculated d_{200}/d_{111} (Figure 3) indicates that the phase distortion has occurred at 3.8 GPa. At this pressure, the silicone oil is solidified but it is not yet stiff enough to markedly distort the Pd nanocubes. With the pressure up to 9.3–12.4 GPa (Figure 2), the solidified silicone oil is stiff enough to produce sufficient shear stress on the Pd nanocubes, resulting in obviously nonhydrostatic conditions (peak broadening) and weakened preferred orientation (peak splitting). That is why the phase distortion above 9.3 GPa becomes the most significant. With pressure continuing up to > 18.8 GPa, the splitting of the 200 peak became observable and the 002 peak could be clearly observed, suggesting that the preferred orientation in the nanocubes weakened under high compression. We did not observe the phase distortion in the Pd nanoplates, which were under the same experimental conditions as the Pd nanocubes. So the observed phase distortion in the Pd nanocubes is unlikely driven by solvent effects or possible oxidization of the surfaces of the Pd nanocrystals.

There are numerous defects in the extended Pd solid. It may break into irregular particles without a special shape and a preferred crystal face when subjected to nonhydrostatic pressure. The fcc to fct distortion would not occur for a bulk solid under these circumstances. However, faceted nanocrystals are very stable and can keep their special shape at high pressures because they are nearly defect free. In the case of hexagonal nanoplates, the external force direction is mainly along the [111] because the exposed crystal face is the (111) and the expected ordered arrangement leads to alignment of the [111] direction of most of the nanoplates parallel to the synchrotron beam and the diamond compression axis. The fcc to fct distortion was not observed up to 20.1 GPa in hexagonal nanoplates because the uniaxial compression occurs along the [111] instead of the [001], but a 3C to

3H distortion is expected to occur in the hexagonal nanoplates under higher pressure (i.e., >50 GPa).

On the basis of our current experimental results and proposed mechanisms, we predict that a similar fcc to fct distortion may be observed in cold-compressed Pt, Ag, and Au nanocubes with {100} as the exposed crystal faces. Also, it might be possible to observe other distortions in transition metal nanocrystals such as a 3C to 3H and a bcc to bct distortion.

In summary, an fcc to fct transformation was observed for the first time in the cold-compressed Pd nanocubes. This novel discovery not only provides new insights into the pressure-induced behavior of faceted nanocrystals of palladium and other noble metals but also gives guidance for finding new phases in close-packed metals.

Acknowledgment. Q.G. is supported by a Director's Postdoctoral Fellowship at Los Alamos National Laboratory (LANL). Y.X. is supported by the NSF (DMR-0451788). This work was supported by the LDRD Program at LANL. LANL is operated by Los Alamos National Security under Department of Energy contract DE-AC52-06NA25396. CHESS is supported by the NSF and NIH/NIGMS via NSF award DMR-0225180. We thank the reviewers for their valuable comments and suggestions.

References

- (1) Chen, C.; Herhold, A. B.; Johnson, C. S.; Alivisatos, A. P. *Science* **1997**, 276, 398.
- (2) Jacobs, K.; Zaziske, D.; Scher, E. C.; Herhold, A. B.; Alivisatos, A. P. *Science* **2001**, 293, 1803.
- (3) Zaziski, D.; Prilliman, S.; Scher, E. C.; Casula, M.; Wickham, J.; Clark, S. M.; Alivisatos, A. P. *Nano Lett.* **2004**, 4, 943.
- (4) Grünwald, M.; Rabani, E.; Dellago, C. *Phys. Rev. Lett.* **2006**, 96, 255701.
- (5) Zhang, H.; Gilbert, B.; Huang, F.; Banfield, J. F. *Nature* **2003**, 424, 1025.
- (6) Gilbert, B.; Huang, F.; Zhang, H.; Waychunas, G. A.; Banfield, J. F. *Science* **2004**, 305, 651.
- (7) Huang, F.; Banfield, J. F. *J. Am. Chem. Soc.* **2005**, 127, 4523.
- (8) Wang, Z.; Daemen, L. L.; Zhao, Y.; Zha, C.; Downs, R. T.; Wang, X.; Wang, Z. L.; Hemley, R. J. *Nat. Mater.* **2005**, 4, 922.
- (9) San-Miguel, A. *Chem. Soc. Rev.* **2006**, 35, 876.
- (10) McMahon, M. I.; Nemes, R. J. *Chem. Soc. Rev.* **2006**, 35, 943.
- (11) fct is equivalent to bct (body-centered tetragonal) except that the cell volume of fct is double that of bct. It is more convenient to use fct than bct for fcc to fct distortions.
- (12) Jona, F.; Marcus, P. M. *Phys. Rev. B* **2002**, 65, 155403–1.
- (13) Ji, X.; Tian, Y.; Jona, F. *Phys. Rev. B* **2002**, 65, 155404–1.
- (14) Lee, S.; Hoffmann, R. J. *Am. Chem. Soc.* **2002**, 124, 4811.
- (15) Xiong, Y.; Chen, J.; Wiley, B. J.; Xia, Y.; Yin, Y.; Li, Z. *Nano Lett.* **2005**, 5, 1237.
- (16) Xiong, Y.; Cai, H.; Wiley, B. J.; Wang, J.; Kim, M. J.; Xia, Y. *J. Am. Chem. Soc.* **2007**, 129, 3665.
- (17) Xiong, Y.; Washio, I.; Chen, J.; Cai, H.; Li, Z.-Y.; Xia, Y. *Langmuir* **2006**, 22, 8563.
- (18) The diamond anvils had ~350 μm culets. The gasket (a T301 stainless-steel) was ~350 μm thick and was pre-indented to ~60 μm . A ~200 μm diameter hole was filled with Pd nanocrystals along with silicone oil (Dow Corning Corporation 200 fluid with a viscosity of 30000 cSt at 25 °C) and ruby, which were used as the pressure-transmitting medium and pressure marker, respectively. An angle-dispersive synchrotron radiation at B2 station of Cornell High Energy Synchrotron Source (CHESS), Cornell University, was used for the X-ray diffraction measurements. A monochromatic beam with a wavelength of 0.55656 Å and a size of ~100 μm was focused on the sample. A MAR345 image plate detector located at ~340 mm distance from the sample served for collecting the X-ray diffraction patterns. Calibration was made using the CeO₂ standard. The collected X-ray diffraction images were integrated by using the Fit2D program (Andy Hammersley, ESRF, 1987–2005).
- (19) Mao, H. K.; Xu, J. A.; Bell, P. M. *J. Geophys. Res.* **1986**, 191, 4673.
- (20) Ragan, D. D.; Clarke, D. R.; Schiferl, D. *Rev. Sci. Instrum.* **1996**, 67, 494.

NL0731217